The reactions of SO_3 with HO_2 radical and $H_2O\cdots HO_2$ radical complex. Theoretical study on the atmospheric formation of HSO_5 and H_2SO_4†

Javier Gonzalez, Miquel Torrent-Sucarrat and Josep M. Anglada*

Received 12th August 2009, Accepted 9th December 2009
First published as an Advance Article on the web 14th January 2010
DOI: 10.1039/b916659a

The influence of a single water molecule on the gas-phase reactivity of the HO_2 radical has been investigated by studying the reactions of SO_3 with the HO_2 radical and with the $H_2O\cdots HO_2$ radical complex. The naked reaction leads to the formation of the HSO_5 radical, with a computed binding energy of 13.81 kcal mol^{-1}. The reaction with the $H_2O\cdots HO_2$ radical complex can give two different products, namely (a) $HSO_5 + H_2O$, which has a binding energy that is computed to be 4.76 kcal mol^{-1} more stable than the $SO_3 + H_2O\cdots HO_2$ reactants ($\Delta(E + ZPE)$ at 0K) and an estimated branching ratio of about 34% at 298K and (b) sulfuric acid and the hydroperoxyl radical, which is computed to be 10.51 kcal mol^{-1} below the energy of the reactants ($\Delta(E + ZPE)$ at 0K), with an estimated branching ratio of about 66% at 298K. The fact that one of the products is H_2SO_4 may have relevance in the chemistry of the atmosphere. Interestingly, the water molecule acts as a catalyst, [as it occurs in (a)] or as a reactant [as it occurs in (b)]. For a sake of completeness we have also calculated the anharmonic vibrational frequencies for HO_2, HSO_5, the $HSO_5\cdots H_2O$ hydrogen bonded complex, H_2SO_4, and two $H_2SO_4\cdots H_2O$ complexes, in order to help with the possible experimental identification of some of these species.

Introduction

Water vapour is very important in the Earth's atmosphere. It is the most abundant atmospheric greenhouse gas[1] and it also has a key role in the chemistry of the atmosphere, showing a plethora of effects. The water molecule reacts with atomic oxygen (O, ^1D) making it the main source of the atmospheric hydroxyl radical,[2] but it can also act as a collision partner, collisionally stabilizing many reaction intermediates. Moreover, the water molecule can form hydrogen-bonded complexes with many atmospheric species, modifying their stability and changing their photochemical features.[3–9] The mean lifetime of such complexes can be quite large and consequently an important fraction of a given molecule can be "kidnapped" by a single water molecule. This occurs, for instance, in the case of the hydroperoxyl radical (HO_2), where about 30% of the total HO_2 concentration can be in form of the $HO_2\cdots H_2O$ complex.[10,11] A single water molecule can have a catalytic effect, as occurs in the HO_2 self-reaction[11,12] or in the oxidation of formaldehyde by the hydroxyl radical[13] and it can also produce a change in the product distribution as predicted for the HCOOH + HO reaction catalyzed by a single water molecule.[14] However, it can act in the opposite direction reducing, for instance, the ability of the hydroxyl radical to oxidize methane.[15] In addition, water itself can act as a reactant, reacting with SO_3 to form sulfuric acid[16–18] or by reacting with carbonyl oxides (intermediates of alkene ozonolysis) producing carboxylic acids or H_2O_2 in a non-radical process.[19–21] In the last case, a second water molecule catalyzes the reaction. All these data clearly suggest that the role that the water vapour plays in the Earth's atmosphere is still not well understood and deserves further research.

In this work we investigate how the water molecule affects the reactivity of the hydroperoxyl radical by studying the reaction between SO_3 and HO_2, and the reaction between SO_3 and the $HO_2\cdots H_2O$ complex as well. This reaction has been chosen because SO_3 is an important intermediate in the atmospheric formation of sulfuric acid and it is formed by oxidation of SO_2 with the hydroxyl radical in a first step (reaction 1) forming the bisulfite radical ($HOSO_2$), followed by reaction of $HOSO_2$ with O_2 (reaction 2),[22] the last can occur through the HSO_5 intermediate radical,[23,24] and is followed also by reaction of SO_3 with water vapour (reaction 3).[16–18,25–29]

$$SO_2 + HO \rightarrow HOSO_2 \quad (1)$$

$$HOSO_2 + O_2 \rightarrow SO_3 + HO_2 \quad (2)$$

$$SO_3 + H_2O \rightarrow H_2SO_4 \quad (3)$$

The reaction of SO_3 with HO_2 is the reverse of reaction 2. It can be important for atmospheric purposes provided that the atmospheric concentration of the hydroperoxyl radical is about 50 times that of HO radical,[2] and this reaction leads to the formation of HSO_5.[30] As far as we know, the reaction of

Departament de Química Biològica i Modelització Molecular, IQAC–CSIC, c/Jordi Girona 18, E-08034 Barcelona, Spain. E-mail: anglada@iqac.csic.es

† Electronic supplementary information (ESI) available: Cartesian coordinates of each stationary point; the harmonic and anharmonic vibrational frequencies and intensities of several compounds of interest; the corresponding rotational constants and Figs. S1–S4 showing the most relevant geometrical parameters of the stationary points investigated. See DOI: 10.1039/b916659a

SO_3 with the $H_2O\cdots HO_2$ complex has not been studied yet, in spite of the fact that its atmospheric concentration is about 15 times higher than that of the OH radical. This reaction can produce the hydrated HSO_5 radical, but it also opens the possibility of forming H_2SO_4, which is of great interest in the chemistry of the atmosphere.

Technical details of the calculations

The geometries for all stationary points have been optimized using the 6-311+G(2df,2p) basis set[31,32] employing the unrestricted density functional Becke's three-parameter and Lee–Yang–Parr functional (B3LYP) method.[33] At each stationary point we have performed harmonic frequency calculations to verify the nature of the corresponding stationary point (minima or transition state), and to provide the zero-point vibrational energy (ZPE) and the thermodynamic contributions to the enthalpy and free energy for T = 298K. In addition, intrinsic reaction coordinate calculations[34–36] have been performed to ensure that the transition states connect the desired reactants and products. For some selected minima of interest, we have also carried out anharmonic frequency calculations in order to help possible experimental identification of these species. The anharmonic corrections have been evaluated at the same level of theory by the second-order perturbative treatment implemented by Barone,[37,38] and the requested third and fourth energy derivatives with respect to normal coordinates have been calculated by numerical differentiation of the analytical Hessians. In recent years, several studies have pointed out the need of considerable computational effort for obtaining accurate geometries and energies of SO_x-containing compounds[39–42] and therefore we have performed additional geometry optimizations at the QCISD/6-311+G(2df,2p) level of theory[43] for the stationary points involved in the SO_3 + HO_2 reaction. The final energies were obtained by performing single-point CCSD(T)[44–47] calculations at the optimized geometries using the more flexible cc-pVTZ basis set and the aug-cc-pVTZ basis set in some cases.[48,49] These calculations were done using the Gaussian 03 program package.[50]

For several stationary points of interest, we have also analyzed the bonding features by using the atoms in molecules (AIM) theory by Bader.[51] This analysis was done over the B3LYP/6-311+G(2df,2p) wave function by using the AIMPAC package.[52] Following the AIM theory, the topological properties of a bond are characterized by the existence of a bond critical point (bcp) and the values of the electron density (ρ_b), its Laplacian ($\nabla^2\rho_b$), and the energy density ($H(r)$) at the bcp. A bond critical point has $\nabla\rho_b = 0$ and the Laplacian of the electronic density describes two different situations. $\nabla^2\rho_b < 0$ indicates that the density is locally concentrated and characterizes a covalent bond. $\nabla^2\rho_b > 0$ indicates that the density is locally depleted and characterizes closed-shell interactions as found in ionic bonds, hydrogen bonds, dative bonds, and van der Waals interactions. For instance, a strong hydrogen bond will be associated with large values of the electron density (around 0.035 a.u.) and positive and large values of the Laplacian of the electron density (around 0.139 a.u.) at the bcp.[53] The energy density (which is the sum of the kinetic and potential energy) determines whether the accumulation of charge is stabilizing (negative values) or destabilizing (positive values).[54–56] The Molden program[57] has been used to visualize the geometrical and wave function features of the different stationary points. Finally, we have also computed the rate constants for two reactions of interest using the Rice–Ramsperger–Kassel–Marcus (RRKM) and conventional transition state theories. In these cases, the UNIMOL and Polyrate programs[58] have been employed.

The reaction between SO_3 and HO_2

Fig. 1 shows a schematic potential energy surface for the SO_3 + HO_2 reaction and the most relevant geometrical parameters of the stationary points are displayed in Fig. 1 and S1 of the ESI.† The relative energies, enthalpies, and free energies are contained in Table 1.

The reaction starts with the formation of the **Cr1** complex, for which our best results provide a computed binding energy of 10.48 kcal mol^{-1}. After the **Cr1** complex the reaction proceeds through **Ts1**, with a very small computed energy barrier (0.80 kcal mol^{-1} at 0K) and forms the HSO_5 (**M1**) radical, which is computed to be 13.81 kcal mol^{-1} more stable than the separate SO_3 + HO_2 reactants. In addition, the $HOSO_2$ + O_2 channel (opposite of reaction 2) is computed to lie 2.82 kcal mol^{-1} below the energy of SO_3 + HO_2. The reliability of our calculations can be also checked by comparing the computed enthalpy of the reaction SO_3 + HO_2 → $HOSO_2$ + O_2 at 298K (−2.69 kcal mol^{-1}, see Table 1) with the experimental value (−0.349 kcal mol^{-1}) obtained taking into account the experimental values of the enthalpies of formation at 298K.[59–62]

From a technical point of view, Figs. 1 and S1 show that the optimized geometries obtained using B3LYP and QCISD

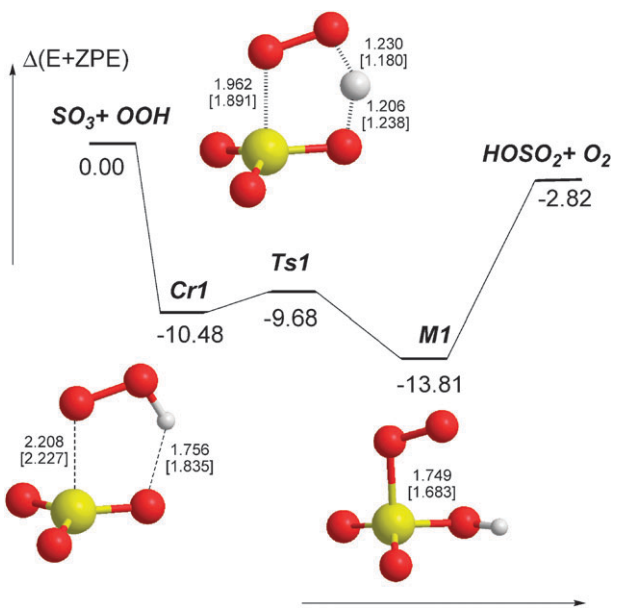

Fig. 1 Schematic potential energy surface for the reaction between SO_3 and HO_2. Distances are in Ångstroms at the B3LYP and QCISD (in brackets) levels of theory. The energy values correspond to calculations at the CCSD(T)/aug-cc-pVTZ//B3LYP/6-311+G(2df,2p) level of theory.

Table 1 Zero-point energies (ZPE in kcal mol^{-1}), Entropies (S in e.u.), and relative energies, energies plus ZPE, enthalpies, and free energies (in kcal mol^{-1}) calculated for the reaction between SO_3 and HO_2[a]

Compound	M[b]	ZPE	S	ΔE	$\Delta(E + ZPE)$	ΔH (298K)	ΔG (298K)
$SO_3 + HO_2$	**A**	16.5	116.1	0.00	0.00	0.00	0.00
	B			0.00	0.00	0.00	0.00
	C			0.00	0.00	0.00	0.00
Cr1	**A**	18.7	81.3	−11.66	−9.44	−10.08	0.30
	B			−12.70	−10.48	−11.12	−0.74
	C			−11.59	−9.28	−9.92	0.46
Ts1	**A**	16.5	76.8	−8.69	−8.67	−9.91	1.81
	B			−9.70	−9.68	−10.92	0.80
	C			−8.96	−8.93	−10.17	1.55
M1	**A**	18.6	79.9	−14.75	−12.64	−13.36	−2.58
	B			−15.93	−13.81	−14.54	−3.76
	C			−14.62	−12.51	−13.23	−2.45
$HOSO_2 + O_2$	**A**	16.1	118.0	−1.33	−1.77	−1.64	−2.22
	B			−2.38	−2.82	−2.69	−3.26
	C			−1.38	−1.82	−1.69	−2.26

[a] In all cases the ZPE, S, and the enthalpic and entropic corrections correspond to calculations at the B3LYP/6-311+G(2df,2p) level of theory. [b] M stands for method: **A**: CCSD(T)/cc-pVTZ//B3LYP/6-311+G(2df,2p); **B**: CCSD(T)/aug-cc-pVTZ//B3LYP/6-311+G(2df,2p), and **C**: CCSD(T)/cc-pVTZ//QCISD/6-311+G(2df,2p).

compare quite well, with differences in the bond lengths smaller than 0.08 Å, and the single-point CCSD(T)/cc-pVTZ energies computed at the optimized geometries obtained at both levels of theory differ by at most 0.27 kcal mol^{-1} (see Table 1).

Complex **Cr1** has very interesting electronic features. It has a five-membered-ring structure and it is stabilized by an interaction between the lone pair of the terminal oxygen of the HO_2 moiety and the sulfur atom of the SO_3 moiety (with a computed S···O bond distance of 2.208 Å at B3LYP and 2.227 Å at QCISD levels of theory), and by a hydrogen-bond interaction between the hydrogen of the HO_2 moiety and one of the oxygen atoms of the SO_3 moiety (with a computed OOH···OSOO bond distance of 1.756 Å computed at B3LYP and 1.835 Å obtained at the QCISD level of theory). Its features have been reported and discussed recently by Solimannejad and co-workers[30] and our results, regarding the optimized geometries and energies, compare quite well with previous works in the literature.[30,63] It is only worth pointing out here that, as it has been shown by Solimannejad and co-workers,[30] the AIM analysis at the bcp of the S···O(OH) interaction presents features of weak interaction character (the topological values are $\rho = 0.0653$, $\nabla^2\rho = 0.1156$, and $H = -0.0100$ a.u.). This complex has C_s symmetry ($^2A''$ electronic state) and the unpaired electron is mainly located on the OO group of the hydroperoxyl radical moiety, in a plane perpendicular to the SO_3 plane, so that it does not participate in the interaction between the HO_2 and SO_3 moieties. **Ts1** has also C_s symmetry ($^2A''$ electronic state) and consequently the unpaired electron does not participate in the reaction either. The process involves the simultaneous transfer of a proton from the HO_2 moiety to one oxygen atom of SO_3 and the formation of a covalent S–O(O) bond in producing **M1** (the topological values of this S–O(O) bond at the corresponding bcp are $\rho = 0.1915$, $\nabla^2\rho = -0.3068$, and $H = -0.1620$ a.u.), pointing out the covalent character of the S–O(O) bond. Thus, the HO_2 radical reacts with SO_3 in the same way as described for the reaction with formaldehyde, where it was shown that the unpaired electron of the radical does not participate in the reaction.[64,65] The product of this reaction (**M1**) is considered to be an important intermediate in the initial nucleation steps of aerosol formation.[63]

The computed geometrical parameters of **M1** are displayed in Fig. S1 of the ESI† and compare quite well with the recently reported values from the literature.[23,41] Because of the importance of the HSO_5 (**M1**) radical intermediate, we have also calculated the corresponding anharmonic frequencies that are contained in Table S3 of the ESI. Our computed values agree quite well with the calculated results reported recently by González-García *et al.*,[41] and a more detailed discussion will be given below. For the sake of completeness we have also considered the possibility that **Cr1** could dissociate into SO_4 + HO. Our calculations predict the formation of these products to be endothermic by 59.5 kcal mol^{-1}, so this process will not occur under atmospheric conditions.

The reaction between SO_3 and the $HO_2\cdots H_2O$ complex

The reaction between SO_3 and the $HO_2\cdots H_2O$ complex can occur in two different ways [(a) and (b)], depending on how the $HO_2\cdots H_2O$ reactant approaches to SO_3. The schematic potential energy surfaces of these reactions have been drawn in Figs. 2 and 3. The energy, enthalpy, and free energy values are collected in Table 2 and the most relevant geometrical parameters of the optimized structures are included in Fig. 2 and 3 and Figs. S2–S4 of the ESI.

The first reaction (a), Fig. 2, begins with the formation of a hydrogen bonded complex (**Cr1a**) formed by interaction between one oxygen atom of SO_3 and the hydrogen of the water moiety in the $H_2O\cdots HO_2$ complex (see Fig. 2 and Fig. S2), having a very small computed binding energy (1.99 kcal mol^{-1}). After a very flat potential energy surface (through **Ts1a**), the **Cr2a** complex is formed, with a predicted binding energy of 11.36 kcal mol^{-1}. Table 2 and Fig. 2 show that the CCSD(T)/cc-pVTZ//B3LYP/6-311+G(2df,2p) energies predict the transition state **TS1a** to lie slightly below the

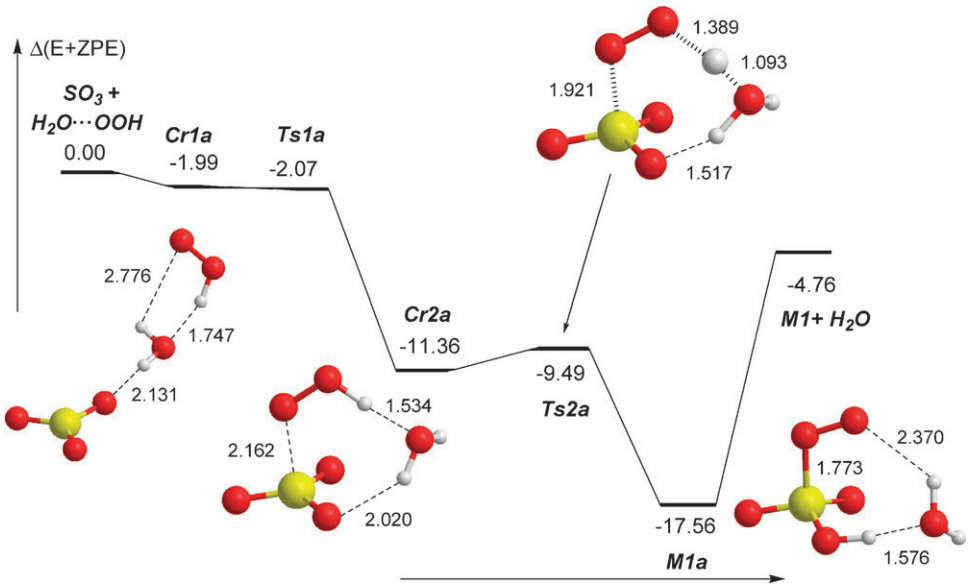

Fig. 2 Schematic potential energy surface for the reaction between SO_3 and $H_2O\cdots HO_2$ leading to the formation of HSO_5 + H_2O. Distances are in Ångstroms at the B3LYP level of theory. The energy values correspond to calculations at the CCSD(T)/cc-pVTZ//B3LYP/6-311+G(2df,2p) level of theory.

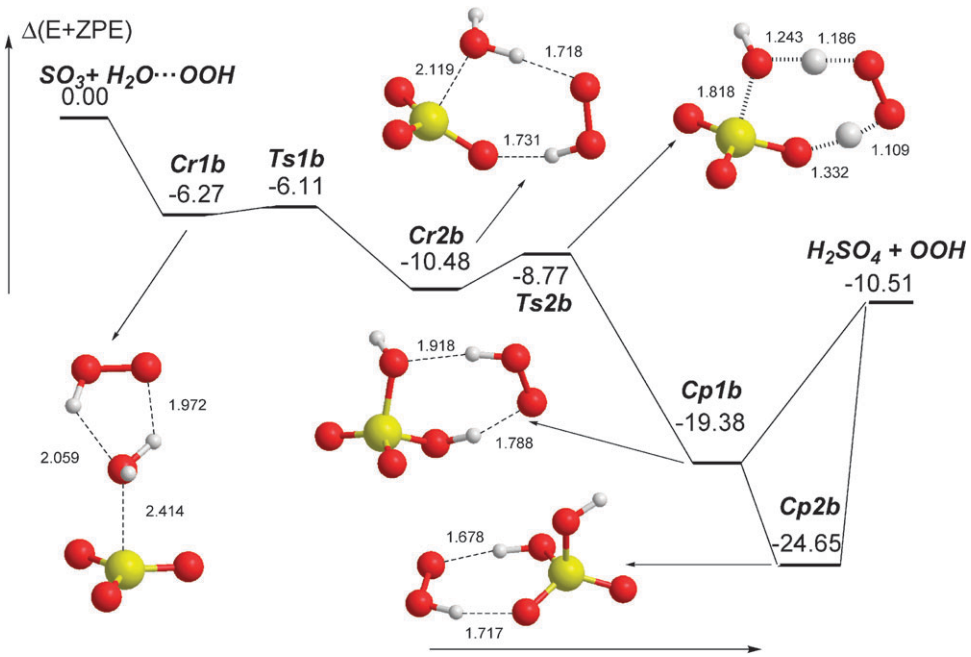

Fig. 3 Schematic potential energy surface for the reaction between SO_3 and $H_2O\cdots HO_2$ leading to the formation of H_2SO_4 + HO_2. Distances are in Ångstroms at the B3LYP level of theory. The energy values correspond to calculations at the CCSD(T)/cc-pVTZ//B3LYP/6-311+G(2df,2p) level of theory.

energy of **Cr1a**, pointing out the difficulty of employing a dual level in predicting the correct energies. Please note that in this case, the imaginary frequency of the transition state is only 10 cm^{-1}, which corresponds to a very flat potential energy surface involving the breakdown of a very weak hydrogen bond in the $H_2O\cdots HO_2$ moiety and the formation of a stronger O···S bond in **Cr2a**. However, when the entropy contributions have been taking into account, **TS1a** lies above **Cr1a** (see ΔG (298K) values in Table 2).

Cr2a has a seven-membered-ring structure and the terminal oxygen of the hydroxyperoxide moiety in $HO_2\cdots H_2O$ bonds the sulfur atom of SO_3, whereas one of the hydrogen atoms of the H_2O moiety links one of the oxygen atoms of SO_3 through a hydrogen bond. The S···O(OH) bond distance is computed to be 2.162 Å and the topological analysis of the wave function (ρ = 0.0709, $\nabla^2\rho$ = 0.1146, and H = −0.0127 a.u.) indicates that it is a weak interaction, with the same features as discussed above for **Cr1**. The reaction proceeds through

Table 2 Zero-point energies (ZPE in kcal mol^{-1}), Entropies (S in e.u.) and relative energies, energies plus ZPE, enthalpies and free energies (in kcal mol^{-1}) calculated for the reaction between SO_3 and the $H_2O\cdots HO_2$ radical complex[a]

Compound	ZPE	S	ΔE	$\Delta(E + ZPE)$	ΔH (298K)	ΔG (298K)
$SO_3 + H_2O\cdots HO_2$	32.5	133.9	0.00	0.00	0.00	0.00
(a) Formation of $HSO_5\cdots H_2O$						
Cr1a	33.0	121.7	−2.50	−1.99	−1.18	2.45
Ts1a	33.0	112.7	−2.56	−2.07	−1.83	4.50
Cr2a	34.3	94.8	−13.18	−11.36	−11.91	−0.25
Ts2a	33.4	86.2	−10.40	−9.49	−11.14	3.09
M1a	34.2	94.4	−19.25	−17.56	−18.16	−6.38
M1 + H_2O	33.0	125.0	−4.30	−4.76	−4.74	−2.09
(b) Formation of H_2SO_4						
Cr1b	33.9	105.2	−9.65	−6.27	−6.20	2.35
Ts1b	33.9	98.2	−7.47	−6.11	−6.59	4.06
Cr2b	34.8	95.8	−12.82	−10.48	−11.13	0.22
Ts2b	32.1	87.1	−8.37	−8.77	−10.49	3.48
Cp1b	35.2	92.3	−22.12	−19.38	−20.33	−7.95
Cp2b	35.3	91.3	−27.41	−24.65	−25.76	−13.08
$H_2SO_4 + HO_2$	33.3	125.8	−11.31	−10.51	−11.09	−8.67

[a] Energies computed at the CCSD(T)/cc-pVTZ//B3LYP/6-311 + G(2df,2p) level of theory. The ZPE, S, and the enthalpic and entropic corrections correspond to calculations at the B3LYP/6-311 + G(2df,2p) level of theory.

Ts2a with a small energy barrier (1.87 kcal mol^{-1}) to form the hydrogen-bonded complex **M1a**.

The process from **Cr2a** to **M1a** involves the formation of a covalent S–O(O) bond and, at the same time, a double proton transfer, from the hydroperoxide moiety to the water moiety and from the water to one oxygen atom of SO_3, so that the unpaired electron of the radical does not participate in the whole reaction. Please note that this reaction corresponds to the reaction described in the previous section, catalyzed by a single water molecule and the product formed (**M1a**) is the hydrated HSO_5 radical. It is computed to be 17.56 kcal mol^{-1}, at 0K, more stable than the reactants ($SO_3 + H_2O\cdots HO_2$ complex). Comparing with the naked reaction discussed above, the addition of a water molecule introduces an extra stabilization of about 5 kcal mol^{-1} in the reaction energy. Here it is also worth pointing out that compound **M1a** has been described very recently in the literature in relation to the early nucleation steps in the aerosol formation.[63]

The second reaction (b) (see Fig. 3 and Figs. S3 and S4) starts with the formation of the **Cr1b** complex, with a quite high computed binding energy of 6.27 kcal mol^{-1}. This complex is held by a van der Waals interaction between the sulfur atom and the oxygen atom of the water moiety in the $H_2O\cdots HO_2$ complex (d(S$\cdots$O) = 2.414 Å). The nature of this interaction is given according to the AIM analysis of the wave function (ρ = 0.0377, $\nabla^2\rho$ = 0.254, and H = −0.0005 a.u.). Then the reaction proceeds through **Ts1b** to form the complex **Cr2b** for which we have computed a binding energy of 10.48 kcal mol^{-1}. Fig. 3 shows that this complex has a seven-membered-ring structure and it is formed by interaction between the sulfur atom of SO_3 and the oxygen of the water moiety in $HO_2\cdots H_2O$ and two hydrogen-bond interactions, one between the hydrogen of the HO_2 moiety and one oxygen atom of SO_3 and the other between one hydrogen atom of water and the terminal oxygen of the hydroperoxide moiety. The S$\cdots$O bond length is computed to be 2.119 Å and the lengths of the two hydrogen bonds are very short (1.731 and 1.718 Å, respectively). It is interesting to point out here that the nature of the S$\cdots$O(H_2) bond in **Cr2b** has the same topological features than those described above for the S$\cdots$O(OH) interaction in **Cr1** and **Cr1a** as indicated by the AIM analysis of the wave function (ρ = 0.0763, $\nabla^2\rho$ = 0.1134, and H = −0.0160 a.u.). The reaction goes on through **Ts2b** in a process that involves the formation of a covalent S–O(H) bond and simultaneously, a double proton transfer, one from the water moiety to the hydroperoxyl moiety and the other from the HO_2 moiety to one oxygen atom of the SO_3 moiety. It is important to remark here that, as above, the whole reaction takes place without the participation of the unpaired electron. The computed energy barrier is 1.71 kcal mol^{-1} and the process leads to the formation of **Cp1b**, which is predicted to lie 19.38 kcal mol^{-1} below the energy of the $SO_3 + H_2O\cdots HO_2$ reactants. **Cp1b** is a hydrogen bonded complex formed between H_2SO_4 and HO_2, so that *this is a new mechanism for the gas-phase formation of sulfuric acid*. The HO_2 radical helps the incorporation of a water molecule to SO_3 in the H_2SO_4 formation process. The reaction mechanism described above clearly shows that this reaction could be easily checked using either isotopically deuterated water or hydroperoxyl radical species. For **Cp1b** we have computed a binding energy of 8.87 kcal mol^{-1} relative to $H_2SO_4 + HO_2$. However, it must be pointed out that this is not the most stable hydrogen-bonded complex formed between sulfuric acid and the hydroperoxyl radical.[66,67] For the sake of completeness, the most stable $H_2SO_4\cdots HO_2$ complex (named as **Cp2b**) is also reported here, for which we have computed a binding energy of 14.14 kcal mol^{-1} relative to $H_2SO_4 + HO_2$ (see Table 2 and Fig. 3 and Fig. S4). At this point we can also tentatively check the reliability of our calculations provided that the enthalpy of formation at 298K is known for some of these species. Taking into account the ΔH_f° (298) of H_2O and HO_2 and the ΔH_r (298) obtained at CCSD(T)/cc-pVTZ//B3LYP/6-311 + fG(2df,2p) of −8.63 kcal mol^{-1} for the formation of the $H_2O\cdots HO_2$ complex, we estimate the ΔH_f° (298) of this complex to be −63.49 kcal mol^{-1}. Combining this value with the experimental ΔH_f° (298) values

of SO_3, H_2SO_4, and HO_2, we estimate a reaction enthalpy for reaction (b) of -14.68 kcal mol^{-1}, which compares well with the -11.09 kcal mol^{-1} computed in this work (see Table 2).[59–62]

Finally, we have also considered the possibility that this reaction could produce H_2O_2 and HSO_4 radical and our calculations predict this channel to be endothermic by 14.0 kcal mol^{-1} (relative to the $SO_3 + H_2O\cdots HO_2$ channel), so that we conclude that these species will not be formed under atmospheric conditions as a consequence of reaction (b).

The results of the present section lead us to conclude that *water introduces different features with respect to the naked reaction, acting as a catalyst, but also producing a new reactivity*.

Infrared spectra

Several of the species investigated in the present work are relevant for atmospheric purposes and this fact has led us to compute their anharmonic frequencies in order to help possible experimental identification. Figs. 4–6 show the anharmonic computed IR spectra, whereas the calculated values, along the computed harmonic frequencies, relative intensities, and a tentative assignation of the vibrational modes, have been included in the ESI (Tables S1–S6). The corresponding harmonic and anharmonic rotational constants have been also included in the ESI (Table S7). In what follows, only the anharmonic frequencies will be considered. In this work we have also considered the anharmonic spectra of H_2SO_4 and the HO_2 radical, which are in a very good agreement with the experimentally observed frequencies;[68–72] given that the differences between the calculated and observed values smaller than 30 cm^{-1} on average.

It is very interesting to compare, in a first step, the IR spectra of the HSO_5 (**M1**) radical with that of the sulfuric acid, that have been drawn in Fig. 4. The dotted line corresponds to the H_2SO_4 spectra and the solid line corresponds to the HSO_5 (**M1**) spectra. Please note that both species have structural similarities (one OH bond in sulfuric acid is substituted by an OO bond in **M1**) and consequently, it is expected that the IR spectra of both compounds show some common features. A look at both spectra (Fig. 4) indicates that there are many similarities, mainly in the region of the most intense bands, what makes it difficult to distinguish between both species. The O–H stretch in **M1** appears in the same region (about 50 cm^{-1} red-shifted with respect to H_2SO_4). Perhaps the clearest way to distinguish between the spectra is to look in the 620–830 cm^{-1} region. The two S–O(H) stretchings in H_2SO_4 are predicted to appear at 781–832 cm^{-1}. For **M1**, the S–O(H) stretching band is predicted to be at 825 cm^{-1} and the S–O(O) stretching band, that could be considered as a signature for this species, is predicted to appear at 622 cm^{-1}.

It is also interesting to compare the predicted spectra for **M1** and **M1a**, in order to see the effect of the water in forming a complex with the HSO_5 radical. The computed IR spectra of both species have been drawn in Fig. 5; the dotted line corresponds to **M1** and the solid line corresponds to **M1a**. The (S)O–H stretching in **M1** is calculated to appear at 3540 cm^{-1}, but this band is predicted to be red-shifted by 780 cm^{-1} as a consequence of the hydrogen-bond interaction in **M1a**, so that it appears at 2761 cm^{-1}, whereas its intensity is predicted to be enhanced almost 12 times. This band can be considered as a signature for identifying the **M1a** radical complex. The two bands in the **M1a** spectra, at 3700 and 3590 cm^{-1}, respectively, correspond to the O–H stretching of the water moiety. The different S–O stretching bands appear between 600 and 1400 cm^{-1} in both compounds and, according to the results of Fig. 5, it would be difficult to distinguish between them. Finally, it is also interesting to note the (H)O–S=O bending band that appears around 450 cm^{-1}

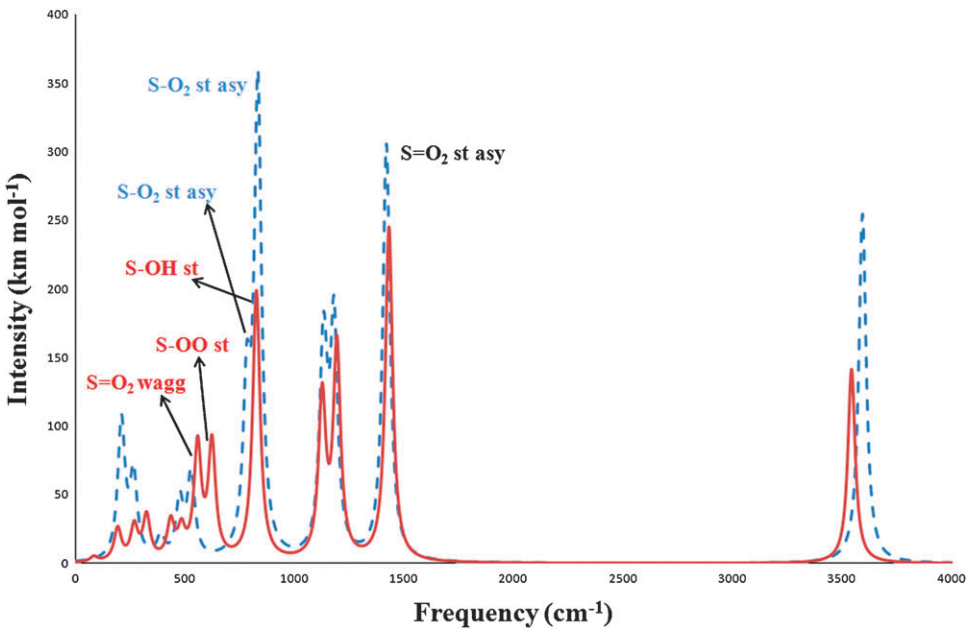

Fig. 4 Computed anharmonic spectra for the H_2SO_4 (dotted line) and **M1** (HSO_5, solid line) compounds, obtained at the B3LYP/6-311+G(2df,2p) level of theory.

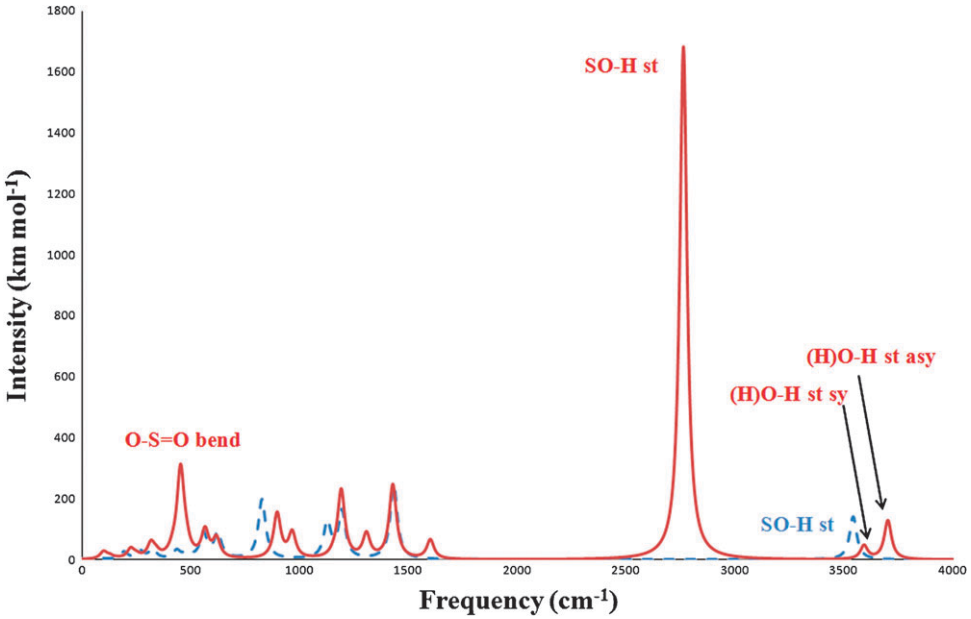

Fig. 5 Computed anharmonic spectra for **M1** (HSO_5, dotted line) and **M1a** ($HSO_5\cdots H_2O$, solid line) compounds, obtained at the B3LYP/6-311 + G(2df,2p) level of theory.

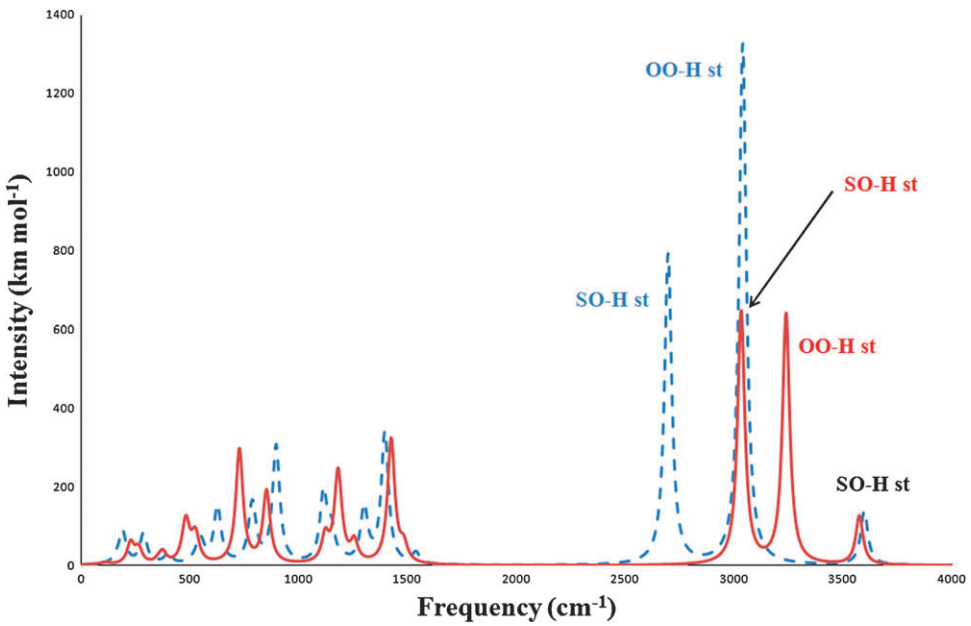

Fig. 6 Computed anharmonic spectra for the $H_2SO_4\cdots H_2O$ complexes (**Cp1b**, dotted line, and **Cp2b**, solid line), obtained at the B3LYP/6-311 + G(2df,2p) level of theory.

can be clearly observed for **M1a**, but not for **M1** (its intensity being computed to be almost unappreciable).

The different kind of interactions between the two $H_2SO_4\cdots HO_2$ complexes (**Cp1b** and **Cp2b**, see Fig. 3) produce differences in the corresponding IR spectra that allow an easy identification. The predicted spectra of both complexes have been drawn in Fig. 6; the solid line corresponds to **Cp1b** and the dotted line corresponds to **Cp2b**, where it can be clearly seen that the main differences are found at the 2700–3300 cm^{-1} region, which is the region where the most O–H stretching bands appear. The **Cp1b** complex is held together by interaction between the terminal oxygen of the HO_2 radical and one of the hydrogen atoms of H_2SO_4 and by interaction between the hydrogen atom of HO_2 and one of the oxygen atoms of the OH groups in sulfuric acid and these two hydrogen bonds produce a red-shift in the corresponding O–H stretching frequencies. Thus, the (O)O–H stretching of the hydroperoxyl radical moiety is predicted to appear at 3237 cm^{-1} with a red-shift of 174 cm^{-1} relative to the free HO_2 radical, whereas one of the S–O(H) stretching appears at

3031 cm^{-1} with a red shift of 558 cm^{-1} relative to the free sulfuric acid. The **Cp2b** complex is held together by interaction between the terminal oxygen of the HO_2 radical and one of the hydrogen atoms of H_2SO_4 and by interaction between the hydrogen atom of HO_2 and one of the oxygen atoms of the S=O groups in sulfuric acid. These hydrogen-bond interactions are stronger than those occurring in **Cp1b** and, consequently the red-shift produced in the corresponding O–H stretching frequencies should be larger. The (O)O–H stretching of the hydroperoxyl radical moiety is predicted to appear at 3038 cm^{-1} with a red-shift of 373 cm^{-1} relative to the free HO_2 radical, whereas one of the S–O(H) stretching bands appears at 2695 cm^{-1} with a red-shift of 894 cm^{-1} relative to the free sulfuric acid. Consequently, the stretching band at 3237 cm^{-1} identifies **Cp1b** and the stretching band at 2695 cm^{-1} identifies **Cp2b**. A detailed comparison between the **Cp2b** and H_2SO_4 spectra can be also found in ref. 67.

Atmospheric relevance of the results

The mechanistic study carried out in the present work has pointed out that the reaction between SO_3 and $H_2O\cdots HO_2$ can lead to the formation of either (a) HSO_5 and/or (b) H_2SO_4. Our results displayed in Table 2 show that, in both cases, the limiting step corresponds to the first transition state (**Ts1a** and **Ts1b**, respectively, see the ΔG (298) values in Table 2) and at this point it is interesting to estimate the competence of both reaction channels, (a) and (b). To do this we have performed RRKM calculations on the limiting steps for the SO_3 + $H_2O\cdots HO_2$ reactions at 298K and our computed values are 2.31×10^{-9} cm^3 $molecule^{-1}$ s^{-1} for reaction (a) and 4.37×10^{-9} cm^3 $molecule^{-1}$ s^{-1} for reaction (b). Then the total rate constant is computed to be 6.68×10^{-9} cm^3 $molecule^{-1}$ s^{-1}. According to these results the branching ratio is computed to be 65.4% for the formation of H_2SO_4 [reaction (b)] and 34.6% for the formation of HSO_5 [reaction (a)]. Similar results are obtained applying the conventional transition state theory at 298K. In this case, the computed values for the rate constants are 1.46×10^{-9} cm^3 $molecule^{-1}$ s^{-1} for reaction (a), 2.92×10^{-9} cm^3 $molecule^{-1}$ s^{-1} for reaction (b), and 4.38×10^{-9} cm^3 $molecule^{-1}$ s^{-1} for the total rate constant. Then the branching ratio is computed to be 66.7% for the formation of H_2SO_4 and 33.3% for the formation of HSO_5, in good agreement with the values obtained from RRKM calculations.

A very important point for atmospheric purposes is to consider whether the reactions investigated in this work may play a role in the chemistry of the Earth's atmosphere. It is well known that the gas-phase formation of H_2SO_4 occurs by the reaction of SO_3 with H_2O (reaction 3) and the atmospheric concentration of water vapour is much higher than that of the hydroperoxyl radical. Experimental results from the literature indicate that the preferred value for the rate constant of reaction 3 is 5.7×10^{4} s^{-1} at 298K and 50% of relative humidity.[73] The inferred upper limits for the bimolecular rate constant at 298K are 2.4×10^{-15} cm^3 $molecule^{-1}$ s^{-1} and 5.7×10^{-15} cm^3 $molecule^{-1}$ s^{-1},[74,75] whereas further experimental studies suggest a second-order dependence of the rate constant with respect to the water vapour, with a rate constant of 2.0–3.0$\times10^{-31}$ cm^6 s^{-1} at 300K.[26,27,29] It has been pointed out in the literature that the gas-phase formation of H_2SO_4 involves the reaction of SO_3 with water dimmers[16–18,26,28] and we will analyze here whether this reaction can compete to any extent with the reactions investigated in the present work. As pointed out above, the estimated rate constant for the SO_3 + $H_2O\cdots HO_2$ reaction is 6.68×10^{-9} cm^3 $molecule^{-1}$ s^{-1}, which is about 10^6 times faster than the inferred experimental value for SO_3 + H_2O reaction (see above). At 298K and with at 50% relative humidity, the gas-phase concentration of H_2O is 3.85×10^{17} molecules cm^{-3} and the gas-phase concentration of $(H_2O)_2$ can be estimated in 1.8×10^{14} molecules cm^{-3}. With a typical gas phase concentration of HO_2 radical of 3×10^{8} molecules cm^{-3} and taking into account that about 30% of it could be found in a complexed form with water,[11] we can estimate a gas-phase concentration of $H_2O\cdots HO_2$ close to 10^8 molecules cm^{-3}, which is about 10^6 times smaller than the concentration of water dimer. This is approximately the same proportion as the relation between the rate constants discussed above and consequently we can conclude that the reactions investigated in the present work could play a role in the chemistry of the Earth's atmosphere.

Conclusions

We have investigated the reactions between SO_3 and the HO_2 radical and with the $H_2O\cdots HO_2$ radical complex and the results of this work lead us to the following conclusions:

(a) The reaction between SO_3 and HO_2 brings about the formation of the HSO_5 radical, but the introduction of a single water molecule, namely the reaction between SO_3 and the $H_2O\cdots HO_2$ radical complex, leads to two different kinds of products, the hydrated HSO_5 radical and H_2SO_4 plus the HO_2 radical. The fact that one of the products of the reaction is H_2SO_4 may have relevance in the chemistry of the Earth's atmosphere.

(b) A single water molecule introduces different features with respect to the naked reaction. The water can act as a catalyst (forming the $HSO_5\cdots H_2O$ complex) or as a reactant, forming sulfuric acid and hydroperoxyl radical.

(c) All elementary reactions investigated in this work, in which the HO_2 radical takes place; occur without participation of the unpaired electron, which seems to be a quite common feature in the gas-phase reactivity of the hydroperoxyl radical.

(d) For H_2SO_4, **M1**, **M1a**, **Cp1b**, **Cp2b**, and HO_2, we have computed the anharmonic frequencies. A comparison of the corresponding calculated spectra will help the identification in possible experimental observation of these species.

(e) Kinetic studies derived from the calculations reported in this work estimate that at 298K, the reaction between SO_3 and $H_2O\cdots HO_2$ will produce approximately 66% of H_2SO_4 and 34% of HSO_5. Our calculations also suggest that this reaction could play a role in the chemistry of the Earth's atmosphere.

Acknowledgements

This research has been supported by the Spanish Dirección General de Investigación Científica y Técnica (DGYCIT, grant CTQ2008-06536/BQU) and by the Generalitat de

Catalunya (Grant 2009SGR01472). The calculations described in this work were carried out at the Centre de Supercomputació de Catalunya (CESCA) and at the CTI-CSIC. J. G. and M.T-S. acknowledge the CSIC for the JAE-DOC contract.

References

1 IPCC, The Intergovernmental Panel on Climate Change. Climate Change 2001: The Scientific basis, http://www.ipcc.ch/ipccreports/tar/wg1/index.htm, Accessed 04-02, 2009.
2 P. S. Monks, *Chem. Soc. Rev.*, 2005, **34**, 376.
3 S. Aloisio and J. S. Francisco, *Acc. Chem. Res.*, 2000, **33**, 825.
4 E. T. Aaltonen and J. S. Francisco, *J. Phys. Chem. A*, 2003, **107**, 1216.
5 J. C. Hansen and J. S. Francisco, *ChemPhysChem*, 2002, **3**, 833.
6 G. Frost and V. Vaida, *J. Geophys. Res.*, 1995, **100**, 18803.
7 V. Vaida, H. G. Kjaergaard, P. E. Hintze and D. J. Donaldson, *Science*, 2003, **299**, 1566.
8 F. M. Tao, K. Higgins, W. Klemperer and D. D. Nelson, *Geophys. Res. Lett.*, 1996, **23**, 1797.
9 R. C. Dunn and J. D. Simon, *J. Am. Chem. Soc.*, 1992, **114**, 4856.
10 S. Aloisio and J. S. Francisco, *J. Phys. Chem. A*, 1998, **102**, 1899.
11 S. Aloisio, J. S. Francisco and R. R. Friedl, *J. Phys. Chem. A*, 2000, **104**, 6597.
12 R. S. Zhu and M. C. Lin, *Chem. Phys. Lett.*, 2002, **354**, 217.
13 E. Vohringer-Martinez, B. Hansmann, H. Hernandez, J. S. Francisco, J. Troe and B. Abel, *Science*, 2007, **315**, 497.
14 J. M. Anglada and J. González, *ChemPhysChem*, 2009, **10**, 3034.
15 M. A. Allodi, M. E. Dunn, J. Livada, K. N. Kirschner and G. C. Shields, *J. Phys. Chem. A*, 2006, **110**, 13283.
16 K. Morokuma and C. Muguruma, *J. Am. Chem. Soc.*, 1994, **116**, 10316.
17 R. Steudel, *Angew. Chem., Int. Ed. Engl.*, 1995, **34**, 1313.
18 T. Loerting and K. R. Liedl, *Proc. Natl. Acad. Sci. U. S. A.*, 2000, **97**, 8874.
19 J. M. Anglada, P. Aplincourt, J. M. Bofill and D. Cremer, *ChemPhysChem*, 2002, **3**, 215.
20 R. Crehuet, J. M. Anglada and J. M. Bofill, *Chem.–Eur. J.*, 2001, **7**, 2227.
21 P. Neeb, F. Sauer, O. Horie and G. K. Moortgat, *Atmos. Environ.*, 1997, **31**, 1417.
22 J. G. Calvert, A. Lazrus, G. L. Kok, B. G. Heikes, J. G. Walega, H. Lind and C. A. Cantrell, *Nature*, 1985, **317**, 27.
23 D. Majumdar, G.-S. Kim, J. Kim, K. S. Oh, J. Y. Lee and K. S. Kima, *J. Chem. Phys.*, 2000, **112**, 723.
24 M. Salonen, T. Kurtén, H. Vehkamäki, T. Berndt and M. Kulmala, *Atmos. Res.*, 2009, **91**, 47.
25 S. K. Ignatov, P. G. Sennikov, A. G. Razuvaev and O. Schrems, *J. Phys. Chem. A*, 2004, **108**, 3642.
26 J. T. Jayne, U. Poschl, Y. M. Chen, D. Dai, L. T. Molina, D. R. Worsnop, C. E. Kolb and M. J. Molina, *J. Phys. Chem. A*, 1997, **101**, 10000.
27 E. R. Lovejoy, D. R. Hanson and L. G. Huey, *J. Phys. Chem.*, 1996, **100**, 19911.
28 T. Loerting and K. R. Liedl, *J. Phys. Chem. A*, 2001, **105**, 5137.
29 C. E. Kolb, J. T. Jayne, D. R. Worsnop, M. J. Molina, R. F. Meads and A. A. Viggiano, *J. Am. Chem. Soc.*, 1994, **116**, 10314.
30 M. Solimannejad, G. Azimi and L. Pejov, *Chem. Phys. Lett.*, 2004, **391**, 201.
31 M. J. Frisch, J. A. Pople and J. S. Binkley, *J. Chem. Phys.*, 1984, **80**, 3265.
32 W. J. Hehre, L. Radom, P. v. R. Schleyer and J. A. Pople, Ab initio *Molecular Orbital Theory*, Wiley, New York, 1986.
33 A. D. Becke, *J. Chem. Phys.*, 1993, **98**, 5648.
34 K. Ishida, K. Morokuma and A. Kormornicki, *J. Chem. Phys.*, 1977, **66**, 2153.
35 C. Gonzalez and H. B. Schlegel, *J. Chem. Phys.*, 1989, **90**, 2154.
36 C. Gonzalez and H. B. Schlegel, *J. Phys. Chem.*, 1990, **94**, 5523.
37 V. Barone, *J. Chem. Phys.*, 2004, **120**, 3059.
38 V. Barone, *J. Chem. Phys.*, 2005, **122**, 014108.
39 D. R. Glowacki, S. K. Reed, M. J. Pilling, D. V. Shalashilin and E. Martinez-Nunez, *Phys. Chem. Chem. Phys.*, 2009, **11**, 963.
40 W. Klopper, D. P. Tew, N. González-Garcia and M. Olzmann, *J. Chem. Phys.*, 2008, **129**, 114308.
41 N. González-García, W. Klopper and M. Olzmann, *Chem. Phys. Lett.*, 2009, **470**, 59.
42 H. Somnitz, *Phys. Chem. Chem. Phys.*, 2004, **6**, 3844.
43 J. A. Pople, M. Head-Gordon and K. Raghavachari, *J. Chem. Phys.*, 1987, **87**, 5968.
44 J. Cizek, *Adv. Chem. Phys.*, 1969, **14**, 35.
45 R. J. Bartlett, *J. Phys. Chem.*, 1989, **93**, 1967.
46 J. A. Pople, R. Krishnan, H. B. Schlegel and J. S. Binkley, *Int. J. Quantum Chem.*, 1978, **14**, 545.
47 K. Raghavachari, G. W. Trucks, J. A. Pople and M. Head-Gordon, *Chem. Phys. Lett.*, 1989, **157**, 479.
48 T. H. J. Dunning, *J. Chem. Phys.*, 1989, **90**, 1007.
49 R. A. Kendall, T. H. Dunning and R. J. Harrison, *J. Chem. Phys.*, 1992, **96**, 6796.
50 M. J. Frisch, G. W. Trucks, H. B. Schlegel, G. E. Scuseria, M. A. Robb, J. R. Cheeseman, J. J. A. Montgomery, T. Vreven, K. N. Kudin, J. C. Burant, J. M. Millam, S. S. Iyengar, J. Tomasi, V. Barone, B. Mennucci, M. Cossi, G. Scalmani, N. Rega, G. A. Petersson, H. Nakatsuji, M. Hada, M. Ehara, K. Toyota, R. Fukuda, J. Hasegawa, M. Ishida, T. Nakajima, Y. Honda, O. Kitao, H. Nakai, M. Klene, X. Li, J. E. Knox, H. P. Hratchian, J. B. Cross, C. Adamo, J. Jaramillo, R. Gomperts, R. E. Stratmann, O. Yazyev, A. J. Austin, R. Cammi, C. Pomelli, J. W. Ocherski, P. Y. Ayala, K. Morokuma, G. A. Voth, P. Salvador, J. J. Dannenberg, V. G. Zakrzewski, S. Dapprich, A. D. Daniels, M. C. Strain, O. Farkas, D. K. Malick, A. D. Rabuck, K. Raghavachari, J. B. Foresman, J. V. Ortiz, Q. Cui, A. G. Baboul, S. Clifford, J. Cioslowski, B. B. Stefanov, G. Liu, A. Liashenko, P. Piskorz, I. Komaromi, R. L. Martin, D. J. Fox, T. Keith, M. A. Al-Laham, C. Y. Peng, A. Nanayakkara, M. Challacombe, P. M. W. Gill, B. Johnson, W. Chen, M. W. Wong, C. Gonzalez and J. A. Pople, *GAUSSIAN 03, Revision C.01*, 2004.
51 R. F. W. Bader, *Atoms in Molecules. A Quantum theory*, Clarendon Press, Oxford, 1995.
52 R. F. W. Bader, *AIMPAC*, downloaded May 2002.
53 P. L. A. Popelier, *J. Phys. Chem. A*, 1998, **102**, 1873.
54 E. Kraka and D. Cremer, in *Theoretical Models of Chemical Bonding. The concept of the Chemical Bond.*, ed. Z. B. Maksic, Springer-Verlag, 1990, vol. 2.
55 R. F. W. Bader, P. L. A. Popelier and T. A. Keith, *Angew. Chem., Int. Ed. Engl.*, 1994, **33**, 620.
56 U. Koch and P. L. A. Popelier, *J. Phys. Chem.*, 1995, **99**, 9747.
57 G. Schaftenaar and J. H. Noordik, *J. Comput.-Aided Mol. Des.*, 2000, **14**, 123.
58 J. C. Corchado, Y.-Y. Chuang, P. L. Fast, J. Villà, W.-P. Hu, Y.-P. Liu, G. C. Lynch, K. A. Nguyen, C. F. Jackels, V. S. Melissas, B. J. Lynch, I. Rossi, E. L. Coitiño, A. Fernandez-Ramos, J. Pu, T. V. Albu, R. Steckler, B. C. Garrett, A. D. Isaacson and D. G. Truhlar, *POLYRATE-version 9.3*, 2002, downloaded October 2009.
59 The experimental values used for the $D_fH°(298)$ are (in kcal mol^{-1}): −57.799 for H_2O, −94.591 for SO_3, −175.70 for H_2SO_4, −92.02 for $HOSO_2$, and 2.94 for HO_2. See ref. 60–62.
60 IUPAC Subcommittee for Gas Kinetic Data Evaluation, http://www.iupac-kinetic.ch.cam.ac.uk/, accessed 29-10-2009.
61 NIST Standard Reference Data Program, http://webbook.nist.gov/chemistry/form-ser.html, accessed 29-10-2009.
62 B. Ruscic, R. E. Pinzon, M. L. Morton, N. K. Srinivasan, M. C. Su, J. W. Sutherland and J. V. Michael, *J. Phys. Chem. A*, 2006, **110**, 6592.
63 T. Kurtén, T. Berndt and F. Stratmann, *Atmos. Chem. Phys.*, 2009, **9**, 3357.
64 J. M. Anglada and V. M. Domingo, *J. Phys. Chem. A*, 2005, **109**, 10786.
65 S. Olivella, J. M. Anglada, A. Sole and J. M. Bofill, *Chem.–Eur. J.*, 2004, **10**, 3404.
66 C. E. Miller and J. S. Francisco, *J. Am. Chem. Soc.*, 2001, **123**, 10387.
67 M. Torrent-Sucarrat, J. M. Anglada and J. M. Luis, *Phys. Chem. Chem. Phys.*, 2009, **11**, 6377.

68 A. Givan, A. Loewenschuss and C. J. Nielsenb, *Phys. Chem. Chem. Phys.*, 1999, **1**, 37.
69 J. Demaison, M. Herman, J. Lievin and H. D. Rudolph, *J. Phys. Chem. A*, 2007, **111**, 2602.
70 J. B. Burkholder, P. D. Hammer, C. J. Howard, J. P. Towle and J. M. Brown, *J. Mol. Spectrosc.*, 1992, **151**, 493.
71 D. D. Nelson and M. S. Zahniser, *J. Mol. Spectrosc.*, 1991, **150**, 527.
72 C. Yamada, Y. Endo and E. Hirota, *J. Chem. Phys.*, 1983, **78**, 4379.
73 R. Atkinson, D. L. Baulch, R. A. Cox, J. N. Crowley, R. F. Hampson, R. G. Hynes, M. E. Jenkin, M. J. Rossi and J. Troe, *Atmos. Chem. Phys.*, 2004, **4**, 1461.
74 T. Reiner and F. Arnold, *J. Chem. Phys.*, 1994, **101**, 7399.
75 X. Y. Wang, Y. G. Jin, M. Suto, L. C. Lee and H. E. Oneal, *J. Chem. Phys.*, 1988, **89**, 4853.